

Dissipative Time Crystals as Passively Protected Oscillating Qubits

Mert Esencan,¹ A. I. Lvovsky,¹ and Berislav Buča^{2,3,1}

¹Clarendon Laboratory, University of Oxford, Parks Road, OX1 3PU, Oxford, United Kingdom

²Université Paris-Saclay, CNRS, LPTMS, 91405, Orsay, France

³Niels Bohr Institute, University of Copenhagen, Blegdamsvej 17, 2100, Copenhagen, Denmark

Protecting information against decoherence in open quantum systems remains a central challenge for quantum computing. In particular, passive error correction schemes have so far been limited to static memories rather than dynamical qubits. We demonstrate that a driven-dissipative bosonic system can encode a persistently oscillating qubit within a noiseless subsystem, realized explicitly in the Bose–Hubbard dimer (BHD). The strong parity symmetry of the model leads to degenerate stationary states. This symmetry is further broken into non-stationary states in the thermodynamic limit, which exhibit persistent oscillations. As the driving force increases, the Liouvillian spectrum of these states features a phase transition. Above the transition point, the non-stationary state encodes quantum information, preserving it in a noiseless subsystem. In addition to global loss that affects both bosonic modes identically, we further add global dephasing and show that the oscillating qubit is preserved. Finally, in order to gain additional physical insight, we study the effect of phase perturbation to both modes and observe that likewise they are passively protected, returning approximately to their initial configurations. These results establish dissipative time-crystalline dynamics as a mechanism for passive protection of dynamical quantum information, enabling autonomously stabilized oscillating qubits.

Introduction.—Open quantum systems lose coherence as they evolve [1]. The decay of dynamical information remains one of the central challenges in building practical quantum computers [2–13]. Significant progress has been made in *active* quantum error correction in theory [2, 14–16], such as surface codes [17–19] and in experiment [20–24] where information is redundantly encoded in the system with ancilla qubits and correction requires active stabilization. While such schemes enable error correction in principle, they require substantial overhead in physical qubits.

An alternative strategy is *passive* error correction, where the dissipative dynamics of the open system autonomously correct errors without active feedback [25]. In these approaches the encoded state may temporarily deviate under the error but naturally relaxes back once the perturbation is removed. Recent theoretical work has explored passive correction in open many-body systems [26–29], and experimental progress has demonstrated its feasibility in cat qubits constructed as the superposition of coherent states [30–35]. However these correction schemes are limited to the protection of *static* quantum memory, not allowing for *dynamical* information processing operations such as quantum gates.

Here we investigate *time crystals* as a medium for passive error correction, utilizing their oscillation as a dynamic feature capable of enabling *in-situ* quantum processing. Time crystals are phases of matter that spontaneously break time-translation symmetry, resulting in persistent oscillations [36]. These phases are robust to external perturbations [37–40] and come in two types. *Discrete time crystals* [41–46] exhibit periodic behavior that is an integer multiple of a time-dependent system drive. *Continuous time crystals* [47–50], on the other hand, exhibit an emerging system response that is not fixed by

the *time-independent* driving and can change continuously as system parameters are varied. More recently, this concept has been studied in the lens of open quantum many-body systems, giving rise to so-called *dissipative time crystals* [51–67]. Time crystals have been experimentally observed in the lab, often on quantum hardware [68–76]. Other types of quantum non-stationarity include many-body scars, synchronization, and Hilbert space fragmentation. [77–108].

In this work we focus on dissipative time crystals. We propose the driven-dissipative Bose-Hubbard dimer (BHD), known to host continuous time crystal phases [109–113], as a platform for quantum information processing. For a certain phase of the BHD we encode dynamical information that can be maintained and passively error-corrected, utilizing the strong parity symmetry of the system [114, 115]. We observe a dissipative phase transition [116, 117] as the driving strength is varied. In the real eigenspectrum, it manifests itself as a level crossing. In the imaginary spectrum, it manifests as an abrupt change in the frequency of the non-stationary state.

Above the transition point, we show that the model hosts a dynamical qubit encoded in a noiseless subsystem that oscillates persistently within a time crystal phase. The noiseless subsystem feature persists in the presence of global dephasing errors, yielding a qubit with a slightly different frequency but similar behavior. The stability of the time crystal phase is manifest in stability to global dephasing errors as we propose the BHD as a possible medium for autonomously correcting quantum gates.

The model and symmetries.—To account for dissipative dynamics, we model the open system with the Lindblad master equation assuming Markovian condi-

tions [1, 118, 119]:

$$\hat{\mathcal{L}}\rho(t) = \frac{\partial \rho}{\partial t} = -i[H, \rho] + \gamma \hat{\mathcal{D}}[L]\rho. \quad (1)$$

The dissipator with strength γ is defined by $\hat{\mathcal{D}}[L]\rho = L\rho L^\dagger - \frac{1}{2}\{L^\dagger L, \rho\}$, where L is the jump operator describing open interaction with the environment.

The driven-dissipative BHD is an open many-body system with two coupled bosonic modes represented by operators a_1 and a_2 . Due to the strong symmetry (defined below), we move to a beam-splitter basis $a_{B,A} = (a_1 \pm a_2)/\sqrt{2}$, which we refer to as the bonding and antibonding modes, respectively. Our Hamiltonian is

$$\begin{aligned} H = & \sqrt{2}F(a_B^\dagger + a_B) + (-\Delta - J)a_B^\dagger a_B + (-\Delta + J)a_A^\dagger a_A \\ & + \frac{U}{2}(a_B^\dagger a_B^\dagger a_B a_B + a_A^\dagger a_A^\dagger a_A a_A + a_B^\dagger a_B^\dagger a_A a_A \\ & + a_B a_B a_A^\dagger a_A^\dagger + 4a_B^\dagger a_B \hat{a}_A^\dagger a_A). \end{aligned} \quad (2)$$

F is the driving amplitude, Δ is the detuning between the drive frequency and resonant frequencies of the two modes, J is the coupling between the modes, and U is the nonlinear interaction strength. The jump operator $L = a_B$ dissipates only the bonding mode, highlighting the strong symmetry of the model. The dissipation is symmetric such that in the lab basis, a_1 and a_2 , have identical couplings to a common reservoir.

To investigate the system in the thermodynamic limit, we take $F \rightarrow \infty$ while keeping $F\sqrt{U}$ fixed, by introducing the scaling parameter N . Thus we redefine the drive and the nonlinearity as $F = \tilde{F}\sqrt{N}$ and $U = \tilde{U}/N$ [120, 121], and increase N to predict the behavior in the thermodynamic limit.

The time dependent density operator is represented by a vector in the doubled-Hilbert space $|\rho(t)\rangle\rangle = e^{\hat{\mathcal{L}}t} |\rho(0)\rangle\rangle = \sum_{j \geq 0}^D e^{\lambda_j t} |r_j\rangle\rangle \langle\langle l_j | \rho(0)\rangle\rangle$, where λ_j are the eigenvalues of the Liouvillian $\hat{\mathcal{L}}$ with left and right eigenoperators $|r_j\rangle\rangle$ and $\langle\langle l_j |$ respectively [1, 122–124].

In generic systems in the absence of special symmetries, the system decays into a unique steady state $r_0 \equiv \rho(\infty)$, as $\lambda_0 = 0$ whereas all other exponents λ_j have negative real parts and lead to the decay of their corresponding states [1]. The BHD, however, hosts a \mathbb{Z}_2 strong parity symmetry $P = \sum_{n_B, n_A \geq 0} (-1)^{n_A} |n_B, n_A\rangle\rangle \langle\langle n_B, n_A |$ where $n_{B,A}$ are the number operators $n_k = a_k^\dagger a_k$ in each mode B or A . P commutes with the Hamiltonian and the jump operators, separately, i.e. $[H, P] = [L, P] = 0$. The strong symmetry of the BHD block-diagonalizes $\hat{\mathcal{L}}$ into four distinct even or odd blocks $\hat{\mathcal{L}} = \hat{\mathcal{L}}_{ee} \oplus \hat{\mathcal{L}}_{eo} \oplus \hat{\mathcal{L}}_{oe} \oplus \hat{\mathcal{L}}_{oo}$ according to the action of P from the left and right on eigenoperators of $\hat{\mathcal{L}}$ [114]. $\hat{\mathcal{L}}_{ee}$ and $\hat{\mathcal{L}}_{oo}$ contain eigenoperators r_{ee} and r_{oo} with zero eigenvalues for all N , representing the degenerate steady states of our system.

We use numerical simulations to find the Liouvillian eigenoperators and the corresponding eigenvalues for

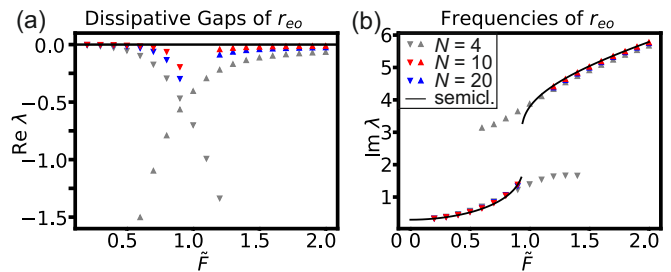


Figure 1. Eigenvalue of r_{eo} for the eigenoperator with the eigenvalue whose real part is closest to zero as a function of the drive \tilde{F} : real (a) and imaginary (b) parts plotted for different N . A phase transition around $\tilde{F} = 0.93$ manifests itself as a level crossing of the dissipative gap (a) and frequency discontinuity (b). Upward/downward triangles represent the eigenoperator above/below the transition point. The full eigenspectra for $N = 3$ were found with exact solvers, whereas sparse solvers were used for $N = 10, 20$ (data for $\tilde{F} = 1.0, 1.1$ not shown as sparse solvers failed near the transition point [125]). In (b), the semiclassical frequency (3) is also shown.

each symmetry sector [125–127]. We work in a truncated two-mode Fock basis $\{|n_B, n_A\rangle\rangle\}$. In our system the antibonding mode remains only weakly populated while the bonding mode carries the large amplitude, so we use an asymmetric Hilbert space truncation $n_A^{\max} \ll n_B^{\max}$ during our numerical studies, which concentrates resources on the relevant sector and allows us to reach large N [125].

As expected [114], we find $\hat{\mathcal{L}}_{ee}$ and $\hat{\mathcal{L}}_{oo}$ to each contain just one eigenoperator with zero eigenvalue, denoted r_{ee} and r_{oo} . For the other two sectors, we select the eigenoperators r_{eo} and r_{oe} for which the real parts of the eigenvalues are closest to zero. As seen in Fig. 1, these real parts of the eigenvalues approach zero with increasing N at both small and large driving amplitudes. The imaginary parts of these eigenvalues however remain nonzero at large N , thus leading to oscillatory behavior and making the system a time crystal [110, 111]. An exception is the neighborhood of $\tilde{F} = 0.93$, where we observe the real parts to deviate from zero, exhibiting a level crossing in both symmetry sectors. The crossing leads to a phase transition, where the non-stationary state that dominates long-time dynamics jumps from the lower frequency branch to the higher frequency branch. We will see next that this transition also captures an abrupt change in quantum information preservation characteristics.

Our quantum simulations are supported by a semiclassical (mean field) approximation elaborated by Lledó *et al.* [110]. This approximation produces a system of coupled differential equations for the amplitudes $\alpha_{A,B} = \langle a_{A,B} \rangle$. Dependent on the parameters, these equations result in monostable or multistable solutions for the bonding mode. We choose a parameter set $J = 1.1$,

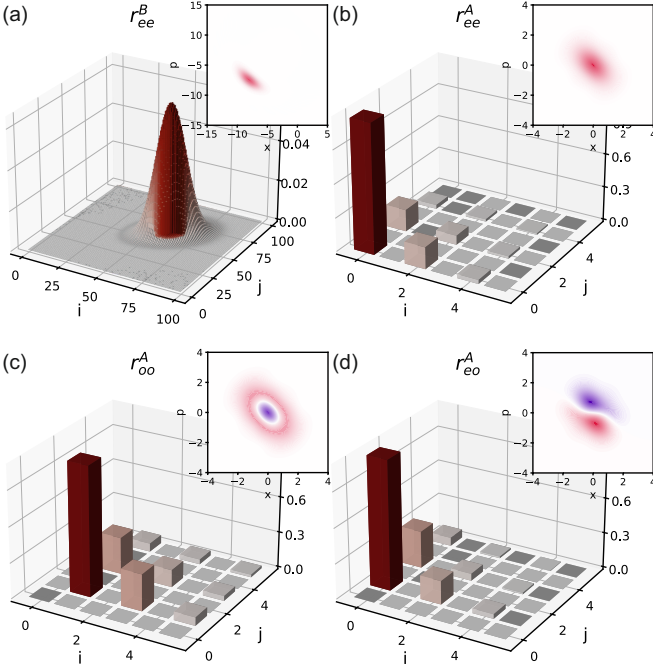


Figure 2. Fock representations (absolute values) and Wigner functions (insets) for the partial traces $r_{ee}^B = \text{Tr}_A(r_{ee})$ (a), $r_{ee}^A = \text{Tr}_B(r_{ee})$ (b), $r_{oo}^A = \text{Tr}_B(r_{oo})$ (c), $r_{eo}^A = \text{Tr}_B(r_{eo})$ (d), of the eigenoperators in the bonding (a) and antibonding (b–d) modes at $\tilde{F} = 1.8$ and $N = 20$. For the bonding mode, the operators r_{ee}^B , r_{oo}^B and r_{eo}^B are very similar to each other [125], hence only r_{ee}^B is displayed in (a). For the Wigner function in (d), the real part is plotted.

$\Delta = 0.8$, $U = 1$, $\gamma = 1$ corresponding to a single stable solution [125]. The solution for the antibonding mode in this case is a persistent oscillation with a microscopic amplitude and the frequency

$$\omega_A = \sqrt{(U|\alpha_B|^2 - \Delta + J)(3U|\alpha_B|^2 - \Delta + J)}. \quad (3)$$

This frequency remarkably matches the imaginary part of the eigenvalue of the selected eigenoperators in r_{ee} and r_{oo} and the phase transition at $\tilde{F} = 0.93$. The eigenoperators themselves [Fig. 2] also exhibit behavior that is consistent with the semiclassical approximation. In the bonding mode [Fig. 2(a)], all eigenoperators are similar to each other and are approximated by a macroscopic coherent state of the amplitude predicted by the semiclassical theory [125]. In the antibonding mode [Fig. 2(b–d)], on the other hand, they are microscopic, approximated by $|0\rangle\langle 0|$, $|1\rangle\langle 1|$, $|0\rangle\langle 1|$ and $|1\rangle\langle 0|$ for r_{ee} , r_{oo} , r_{eo} and r_{oe} , respectively. The Wigner functions of r_{eo} and r_{oe} spin in the phase space of the antibonding mode with their corresponding eigenfrequencies, which are close to ω_A .

Noiseless subsystem as a phase.—To explore the quantum information dynamics of the system, we consider the density operator of the system in vector form as

$$\rho(t) = b|r_{ee}\rangle + (1-b)|r_{oo}\rangle + c(t)|r_{eo}\rangle + c^*(t)|r_{oe}\rangle, \quad (4)$$

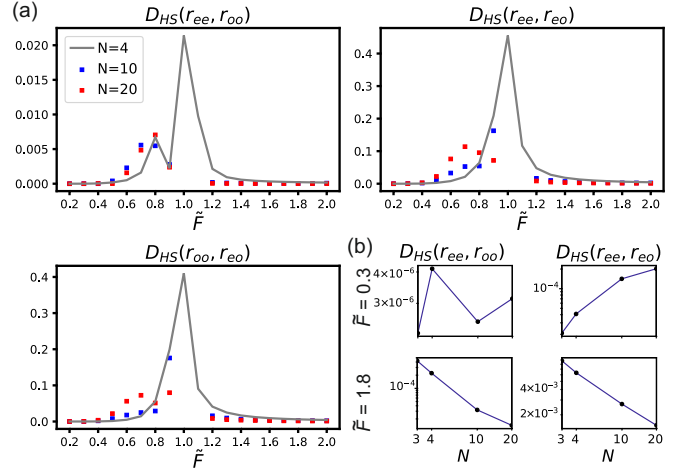


Figure 3. (a) Hilbert–Schmidt (HS) distances between pairs of right eigenoperators as functions of the normalized system drive strength \tilde{F} for $N = 4, 10, 20$. At driving strengths larger than $\tilde{F} = 0.93$ the eigenoperators approach one another towards the thermodynamic limit, indicating the emergence of a NS that encodes a qubit. (b) Scaling of HS distances at representative driving strength values, demonstrating that the subsystem becomes asymptotically noiseless in the large N limit above the transition point. The exponential scaling of the distances plotted implies that the pairwise distances of all eigenoperators $\{r_{oo}, r_{ee}, r_{eo}, r_{oe}\}$ scale similarly because r_{eo} and r_{oe} are Hermitian conjugates of each other.

which is a non-stationary state with persistent oscillations in the thermodynamic limit, with the classical probability $|b|^2$ and the coherence $c(t)$ preserved up to a complex phase oscillation in $c(t)$. However, this state represents a qubit only if it can be represented in the form

$$\rho(t) = \rho_Q \otimes M, \quad \text{where } \rho_Q = \begin{pmatrix} b & c^*(t) \\ c(t) & 1-b \end{pmatrix} \quad (5)$$

and M is an arbitrary density matrix and ρ_Q is referred to as *noiseless subsystem* (NS) [5, 8, 128–131].

To demonstrate the NS, we need to show that the matrices z_{ee} , z_{oo} , z_{eo} and z_{oe} of r_{ee} , r_{oo} , r_{eo} and r_{oe} , respectively, are equal up to a coefficient in some basis. To this end, we choose the basis that diagonalizes r_{ee} and r_{oo} . We then compute the normalized *Hilbert-Schmidt (HS) distance*:

$$D_{HS}(z_{ij}, z_{i'j'}) = 1 - \left\langle \frac{z_{ij}}{\langle z_{ij}, z_{ij} \rangle}, \frac{z_{i'j'}}{\langle z_{i'j'}, z_{i'j'} \rangle} \right\rangle. \quad (6)$$

As evidenced by Fig. 3, $\lim_{N \rightarrow \infty} D_{HS}(z_{ij}, z_{ij}) = 0$ for $\tilde{F} > 0.93$, meaning that the system begins to host a noiseless qubit in the thermodynamic limit. Below the phase transition point, the N -scaling direction is opposite and no NS exists.

One may be tempted to hypothesize that the NS is contained within the antibonding mode as this mode is not subjected to dissipation. If this were the case, the partial

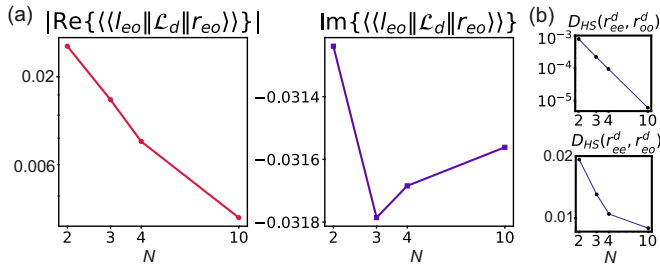


Figure 4. (a) Real and imaginary parts of the leading order of the dephasing perturbation with the rate $\gamma/10$. (b) Scaling of HS distances at $\tilde{F} = 1.8$. Both the real part in (a) and the distances in (b) exhibit exponential decay, indicating existing of an NS in spite of dephasing.

traces r_{ij}^A [Fig. 2(b-d)] would be pure states. However, this is not the case as the purity of these partial traces tend to a constant value for increasing N [125]. Although the antibonding mode does not experience dissipation directly, it is strongly coupled to the dissipating bonding mode, hence the quantum dynamics of the two modes is significantly entangled and the observed NS is a consequence of much more complex dynamics.

Passive Dephasing Protection.— An important question is what happens to the noiseless qubit as the system is subjected to dephasing, a common decoherence mechanism [1, 9, 132]. For our analysis, we investigate global dephasing and add to our dissipator an extra collective Lindblad jump operator, $L_d = a_B^\dagger a_B + a_A^\dagger a_A$. This also has the benefit of preserving the strong symmetry.

Let us first treat dephasing as a perturbation to the non-stationary states. A similar study was done for cat qubits to show dephasing protection of quantum memory [133]. In Fig. 4, we plot the real part of the leading order of the dephasing perturbation to our unperturbed eigenvalue, $\delta_\lambda = \langle\langle l_j | \hat{\mathcal{L}}_d | r_j \rangle\rangle$, where $\hat{\mathcal{L}}_d = \mathcal{D}[L_d]$ [125]. The change in the real part of λ_{eo} diminishes with N , demonstrating that the state does not decay in the thermodynamic limit. We note that the imaginary part of the leading order δ_λ is nonzero, accounting for a small frequency shift. Hence, under persistent global dephasing, the oscillatory qubit remains preserved in the leading perturbation theory order.

To complement the perturbation analysis, we repeat the noiseless subsystem scaling analysis in the presence of dephasing, investigating the eigenoperators of the perturbed Liouvillian $\hat{\mathcal{L}} + \frac{\gamma}{10}\hat{\mathcal{L}}_d$ in Fig. 4 (b). The behavior closely mirrors the undepleted case [Fig. 3 (b)] the HS overlaps between the four symmetry-sector eigenoperators again decrease with increasing N . Thus, although dephasing alters the eigenoperators [125], the noiseless subsystem is not prevented by dephasing.

To gain further physical insight into this observation, we apply macroscopic instantaneous phase kicks to both modes, with $\phi = 1$, and evolve the system with quantum

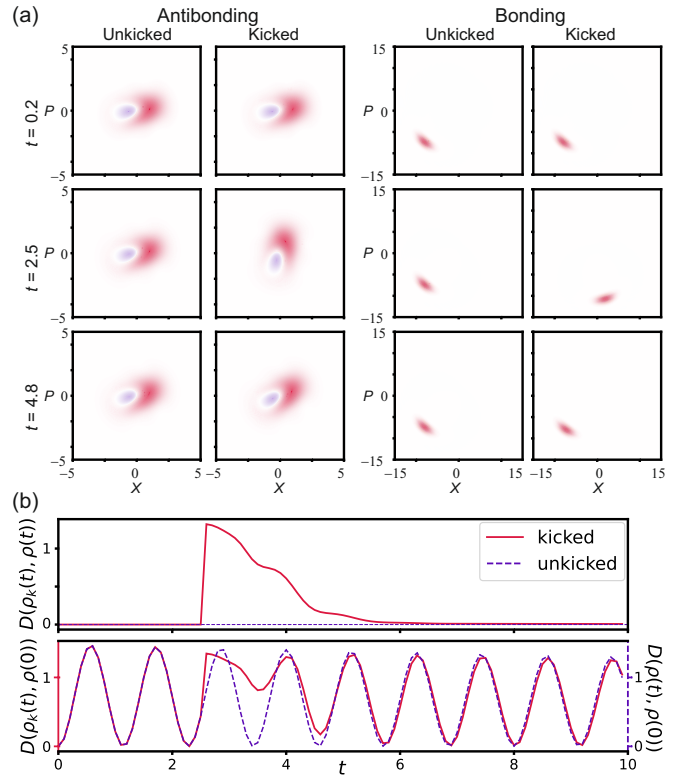


Figure 5. Evolution of the state (4) initialized with $b = c(0) = 1/2$ with $\tilde{F} = 1.8$ at $N = 20$ after an instantaneous phase kick at $t = 2.5$ of magnitude $\delta\phi = 1$ in the rotating frame of reference for partial traces over bonding and antibonding modes. Bonding mode recovers due to dissipative dynamics. The complex amplitude of the bonding mode is coupled to the phase of the antibonding mode, pulling the phase back during its evolution. (a) Snapshots of Wigner functions. (b) Distances of the evolving kicked and unkicked states with respect to the unkicked state $\rho(t)$ (top) and $\rho(0)$ (bottom).

jump trajectories [134]. As seen in Fig. 5(b), the state $\rho_{\text{error}}(t)$ returns approximately to the unkicked state $\rho(t)$, as the distance between these states $D(\rho_{\text{error}}(t), \rho(t)) = \text{Tr}[(\rho(t) - \rho_{\text{error}}(t))^\dagger (\rho(t) - \rho_{\text{error}}(t))]$ diminishes during the evolution after the kick, with long-time sinusoidal behavior for both $\hat{\mathcal{L}}_d$ and $\hat{\mathcal{L}}$. To illustrate the oscillatory behavior of the time crystal, we also plot the distances $D(\rho(t), \rho_0(t))$ and $D(\rho_{\text{error}}(t), \rho_0(t))$ in Fig.5(b)

We visualize this evolution via Wigner functions in Fig. 5(a); see also an animation in the repository [126]. The return of the bonding mode to its initial configuration can be understood semiclassically, since for the system parameters chosen there is one unique solution to the bonding state due to dissipative dynamics. What is more remarkable, though, is that the antibonding mode also recovers from the kick. This is because the bonding mode, in the process of recovering its phase, also temporarily changes its amplitude due to the self-phase modulation term $a_B^\dagger a_B^\dagger a_B a_B$ in the Hamiltonian (2) [125]. The cross-phase modulation term $a_B^\dagger a_B \hat{a}_A^\dagger a_A$ then causes this mod-

ified amplitude to affect the phase of the antibonding mode, correcting it to nearly its initial value. In other words, the classical bonding mode acts as a “guardian” to the quantum antibonding mode.

Discussion and outlook.— We have demonstrated that the driven-dissipative BHD goes through a dynamical transition relevant for quantum information storage at a critical driving strength magnitude. During this transition, the dominant non-stationary state jumps from a low frequency branch to a high frequency branch. The high frequency branch supports a qubit encoded in the noiseless subsystem of the BHD.

Furthermore, we provide evidence that the BHD non-stationary states are protected against dephasing errors due to dissipative dynamics. More specifically, the system recovers after instantaneous phase kicks, supported by dissipation and nonlinear interaction terms. By choosing appropriate system parameters, one can therefore encode a persistently oscillating noiseless qubit, passively protecting against global dephasing errors.

With such protection mechanisms, strong symmetric open systems can provide a platform for controlled phase shifts. As frequency of the oscillations can be controlled through system parameters, single-qubit gates can be implemented by a judiciously constructed detuned pulse sequence. Time crystals have been suggested to be utilized as NOT gates in a recent colloquium [135]. In our work controlled rotations provide a potential pathway toward implementing non-Clifford phase gates within a dissipatively stabilized setting. A systematic gate-level construction will be addressed in future research.

The emergence of the noiseless oscillating qubit can be understood as a separation of scales. The antibonding mode is not fully captured by the semiclassical treatment since it is weakly populated, quantum, and microscopic. The bonding mode, however, is macroscopic and semiclassical, relaxing to a single stable point under dissipation while protecting the antibonding mode from dephasing and loss. In other words, the antibonding mode and the noiseless subsystem is a *dissipative phase* [136]. The kick dynamics then provide a direct visualization of the protection mechanism: the bonding mode’s dissipative recovery pulls the antibonding phase back through nonlinear coupling, restoring the encoded coherence after a macroscopic phase perturbation.

We focus on global dephasing and loss, since only symmetric noise preserves the strong-parity blocks of the Liouvillian; any mode-asymmetric (local) dephasing would mix these sectors and destroy the noiseless subsystem protection. However this restriction is compatible with experiments where both modes naturally couple to a common reservoir, making global dephasing the dominant error channel. These could be probed in contemporary photonic platforms, including driven Kerr resonators [137] and cat-qubit architectures [138, 139], where parity protection, engineered dissipation, and high-coherence

bosonic modes are readily available. Strong symmetry constraints similar to those in the BHD also arise in superconducting circuits and spin ensembles with global dissipation [140], suggesting several experimentally accessible routes for realizing noiseless dynamical subsystems.

Acknowledgments.— We thank C. Lledó, S. Lieu, and D. Sels for their discussions. We are also grateful for the conversation with K. Müller that led to new computational insights. B.B. acknowledges funding by the French National Research Agency (ANR) under Project No. ANR-24-CPJ1-0150-01 and the research grant (No. 42085) from Villum Fonden. A.L.’s research is supported by EPSRC Standard Grant EP/Y020596/1 and the EPSRC Impact Acceleration Account Award EP/X525777/1. B.B. would like to dedicate this article to his loved, talented, and lovely wife Vendi who has always loved, supported, and assisted him as his unsung hero, especially during the most difficult times *when the dreams run dry*.

-
- [1] H.-P. Breuer and F. Petruccione, *The Theory of Open Quantum Systems* (Oxford University Press, 2007).
 - [2] P. W. Shor, Scheme for reducing decoherence in quantum computer memory, *Physical Review A* **52**, R2493 (1995).
 - [3] W. G. Unruh, Maintaining coherence in quantum computers, *Physical Review A* **51**, 992.
 - [4] I. Chuang, R. Laflamme, P. Shor, and W. Zurek, Quantum computers, factoring, and decoherence, *Science* **270**, 1633, quant-ph/9503007.
 - [5] G. Palma, K. Suominen, and A. Ekert, Quantum computers and dissipation, *Proceedings of the Royal Society of London. Series A: Mathematical, Physical and Engineering Sciences* **452**, 567 (1996).
 - [6] E. Knill, R. Laflamme, and W. H. Zurek, Resilient quantum computation: Error models and thresholds, *Proceedings of the Royal Society of London. Series A: Mathematical, Physical and Engineering Sciences* **454**, 365, quant-ph/9702058.
 - [7] L. Viola, E. Knill, and S. Lloyd, Dynamical decoupling of open quantum systems, *Physical Review Letters* **82**, 2417.
 - [8] E. Knill, R. Laflamme, and L. Viola, Theory of Quantum Error Correction for General Noise, *Physical Review Letters* **84**, 2525 (2000).
 - [9] W. H. Zurek, Decoherence, einselection, and the quantum origins of the classical, *Reviews of Modern Physics* **75**, 715 (2003).
 - [10] D. Suter and G. A. Álvarez, Colloquium: Protecting quantum information against environmental noise, *Reviews of Modern Physics* **88**, 041001.
 - [11] L. Egan, D. M. Debroy, C. Noel, A. Risinger, D. Zhu, D. Biswas, M. Newman, M. Li, K. R. Brown, M. Cetina, and C. Monroe, Fault-tolerant control of an error-corrected qubit, *Nature* **598**, 281.

- [12] L. Ding, J. Fan, and X. Qiu, Universally robust control of open quantum systems, npj Quantum Information 10.1038/s41534-025-01166-y.
- [13] M. A. Nielsen and I. L. Chuang, Quantum Computation and Quantum Information: 10th Anniversary Edition (2010).
- [14] A. M. Steane, Error Correcting Codes in Quantum Theory, Physical Review Letters **77**, 793 (1996).
- [15] D. Gottesman, Theory of fault-tolerant quantum computation, Physical Review A **57**, 127 (1998).
- [16] B. M. Terhal, Quantum error correction for quantum memories, Reviews of Modern Physics **87**, 307.
- [17] E. Dennis, A. Kitaev, A. Landahl, and J. Preskill, Topological quantum memory, Journal of Mathematical Physics **43**, 4452 (2002).
- [18] A. G. Fowler, M. Mariantoni, J. M. Martinis, and A. N. Cleland, Surface codes: Towards practical large-scale quantum computation, Physical Review A **86**, 032324 (2012).
- [19] S. Krinner, N. Lacroix, A. Remm, A. Di Paolo, E. Genois, C. Leroux, C. Hellings, S. Lazar, F. Swiadek, J. Herrmann, G. J. Norris, C. K. Andersen, M. Müller, A. Blais, C. Eichler, and A. Wallraff, Realizing repeated quantum error correction in a distance-three surface code, Nature **605**, 669.
- [20] R. Barends, J. Kelly, A. Megrant, A. Veitia, D. Sank, E. Jeffrey, T. C. White, J. Mutus, A. G. Fowler, B. Campbell, Y. Chen, Z. Chen, B. Chiaro, A. Dunsworth, C. Neill, P. O'Malley, P. Roushan, A. Vainsencher, J. Wenner, A. N. Korotkov, A. N. Cleland, and J. M. Martinis, Superconducting quantum circuits at the surface code threshold for fault tolerance, Nature **508**, 500 (2014).
- [21] J. Kelly, R. Barends, A. G. Fowler, A. Megrant, E. Jeffrey, T. C. White, D. Sank, J. Y. Mutus, B. Campbell, Y. Chen, Z. Chen, B. Chiaro, A. Dunsworth, I.-C. Hoi, C. Neill, P. J. J. O'Malley, C. Quintana, P. Roushan, A. Vainsencher, J. Wenner, A. N. Cleland, and J. M. Martinis, State preservation by repetitive error detection in a superconducting quantum circuit, Nature **519**, 66 (2015).
- [22] N. Ofek, A. Petrenko, R. Heeres, P. Reinhold, Z. Leghtas, B. Vlastakis, Y. Liu, L. Frunzio, S. M. Girvin, L. Jiang, M. Mirrahimi, M. H. Devoret, and R. J. Schoelkopf, Extending the lifetime of a quantum bit with error correction in superconducting circuits, Nature **536**, 441 (2016).
- [23] Z. Chen, K. J. Satzinger, J. Atalaya, A. N. Korotkov, A. Dunsworth, D. Sank, C. Quintana, M. McEwen, R. Barends, P. V. Klimov, S. Hong, C. Jones, A. Petukhov, D. Kafri, S. Demura, B. Burkett, C. Gidney, A. G. Fowler, A. Paler, H. Putterman, I. Aleiner, F. Arute, K. Arya, R. Babbush, J. C. Bardin, A. Bengtsson, A. Bourassa, M. Broughton, B. B. Buckley, D. A. Buell, N. Bushnell, B. Chiaro, R. Collins, W. Courtney, A. R. Derk, D. Eppens, C. Erickson, E. Farhi, B. Foxen, M. Giustina, A. Greene, J. A. Gross, M. P. Harrigan, S. D. Harrington, J. Hilton, A. Ho, T. Huang, W. J. Huggins, L. B. Ioffe, S. V. Isakov, E. Jeffrey, Z. Jiang, K. Kechedzhi, S. Kim, A. Kitaev, F. Kostritsa, D. Landhuis, P. Laptev, E. Lucero, O. Martin, J. R. McClean, T. McCourt, X. Mi, K. C. Miao, M. Mohseni, S. Montazeri, W. Mruczkiewicz, J. Mutus, O. Naaman, M. Neeley, C. Neill, M. Newman, M. Y. Niu, T. E. O'Brien, A. Opremcak, E. Ostby, B. Pató, N. Redd, P. Roushan, N. C. Rubin, V. Shvarts, D. Strain, M. Szalay, M. D. Trevithick, B. Villalonga, T. White, Z. J. Yao, P. Yeh, J. Yoo, A. Zalcman, H. Neven, S. Boixo, V. Smelyanskiy, Y. Chen, A. Megrant, J. Kelly, and Google Quantum AI, Exponential suppression of bit or phase errors with cyclic error correction, Nature **595**, 383 (2021).
- [24] V. V. Sivak, A. Eickbusch, B. Royer, S. Singh, I. Tsioutsios, S. Ganjam, A. Miano, B. L. Brock, A. Z. Ding, L. Frunzio, S. M. Girvin, R. J. Schoelkopf, and M. H. Devoret, Real-time quantum error correction beyond break-even, Nature **616**, 50.
- [25] F. Verstraete, M. M. Wolf, and J. I. Cirac, Quantum computation, quantum state engineering, and quantum phase transitions driven by dissipation, 0803.1447 [quant-ph].
- [26] S. Lieu, R. Belyansky, J. T. Young, R. Lundgren, V. V. Albert, and A. V. Gorshkov, Symmetry breaking and error correction in open quantum systems, Physical Review Letters **125**, 240405 (2020), arXiv:2008.02816 [cond-mat, physics:physics, physics:quant-ph].
- [27] S. Lieu, Y.-J. Liu, and A. V. Gorshkov, Candidate for a passively-protected quantum memory in two dimensions (2022), arXiv:2205.09767 [cond-mat, physics:quant-ph].
- [28] Y.-J. Liu and S. Lieu, Dissipative phase transitions and passive error correction, Physical Review A **109**, 022422 (2024).
- [29] N. Suri, J. Saied, and D. Venturelli, Uniformly decaying subspaces for error-mitigated quantum computation, Physical Review A **110**, 042621 (2024).
- [30] G. S. Thekkadath, B. A. Bell, I. A. Walmsley, and A. I. Lvovsky, Engineering Schrödinger cat states with a photonic even-parity detector, Quantum **4**, 239 (2020), arXiv:1908.10314 [quant-ph].
- [31] Z. Leghtas, S. Touzard, I. M. Pop, A. Kou, B. Vlastakis, A. Petrenko, K. M. Sliwa, A. Narla, S. Shankar, M. J. Hatridge, M. Reagor, L. Frunzio, R. J. Schoelkopf, M. Mirrahimi, and M. H. Devoret, Confining the state of light to a quantum manifold by engineered two-photon loss, Science **347**, 853, 1412.4633 [quant-ph].
- [32] R. Lescanne, M. Villiers, T. Peronin, A. Sarlette, M. Delbecq, B. Huard, T. Kontos, M. Mirrahimi, and Z. Leghtas, Exponential suppression of bit-flips in a qubit encoded in an oscillator, Nature Physics **16**, 509.
- [33] A. Grimm, N. E. Frattini, S. Puri, S. O. Mundhada, S. Touzard, M. Mirrahimi, S. M. Girvin, S. Shankar, and M. H. Devoret, Stabilization and operation of a kerr-cat qubit, Nature **584**, 205.
- [34] J. Guillaud and M. Mirrahimi, Repetition Cat Qubits for Fault-Tolerant Quantum Computation, Physical Review X **9**, 041053 (2019), arXiv:1904.09474 [cond-mat, physics:quant-ph].
- [35] C. Chamberland, K. Noh, P. Arrangoiz-Arriola, E. T. Campbell, C. T. Hann, J. Iverson, H. Putterman, T. C. Bohdanowicz, S. T. Flammia, A. Keller, G. Refael, J. Preskill, L. Jiang, A. H. Safavi-Naeini, O. Painter, and F. G. S. L. Brandão, Building a fault-tolerant quantum computer using concatenated cat codes, PRX Quantum **3**, 010329 (2022), arXiv:2012.04108 [quant-ph].
- [36] F. Wilczek, Quantum time crystals, Physical Review Letters **109**, 160401.
- [37] V. Khemani, A. Lazarides, R. Moessner, and S. Sondhi, Phase structure of driven quantum systems, Physical

- Review Letters **116**, 250401.
- [38] T. L. Heugel, A. Eichler, R. Chitra, and O. Zilberberg, The role of fluctuations in quantum and classical time crystals, *SciPost Physics Core* **6**, 053.
- [39] Y. Li, X. Li, and J. Jin, Quantum nonstationary phenomena of spin systems in collision models, *Physical Review A* **107**, 042205.
- [40] Y. J. Zhao, J. E. Moore, J. Thingna, and C. W. Wächtler, Quantum synchronization of perturbed oscillating coherences, 2510.11601 [quant-ph].
- [41] D. V. Else, B. Bauer, and C. Nayak, Floquet time crystals, *Physical Review Letters* **117**, 090402.
- [42] F. Gambetta, F. Carollo, M. Marcuzzi, J. Garrahan, and I. Lesanovsky, Discrete time crystals in the absence of manifest symmetries or disorder in open quantum systems, *Physical Review Letters* **122**, 015701.
- [43] H. Zhao, F. Mintert, and J. Knolle, Floquet time spirals and stable discrete-time quasicrystals in quasiperiodically driven quantum many-body systems, *Phys. Rev. B* **100**, 134302 (2019).
- [44] S. Sarkar and Y. Dubi, Time crystals from single-molecule magnet arrays, *ACS Nano* **18**, 27988.
- [45] P. Kongkhambut, J. G. Cosme, J. Skulte, M. A. Moreno Armijos, L. Mathey, A. Hemmerich, and H. Keßler, Observation of a phase transition from a continuous to a discrete time crystal, *Reports on Progress in Physics* **87**, 080502 (2024).
- [46] L. Fernandes, J. Tindall, and D. Sels, Nonperturbative decay of bipartite discrete time crystals, *Physical Review B* **111**, L100304 (2025).
- [47] D. Dreon, A. Baumgärtner, X. Li, S. Hertlein, T. Esslinger, and T. Donner, Self-oscillating pump in a topological dissipative atom-cavity system, *Nature* **608**, 494 (2022).
- [48] M. Krishna, P. Solanki, M. Hajdušek, and S. Vinjanampathy, Measurement-induced continuous time crystals, *Physical Review Letters* **130**, 150401.
- [49] H. Wang and J. Wang, Time-crystal phase emerging from a qubit network under unitary random operations, *Physical Review A* **108**, 012209 (2023).
- [50] S. Yang, Z. Wang, L. Fu, and J. Jie, Emergent continuous time crystal in dissipative quantum spin system without driving, *Communications Physics* **8**, 114 (2025).
- [51] J. Marino and S. Diehl, Quantum dynamical field theory for non-equilibrium phase transitions in driven open systems, *Physical Review B* **94**, 085150 (2016), arXiv:1606.00452 [cond-mat].
- [52] O. A. Castro-Alvaredo, B. Doyon, and T. Yoshimura, Emergent Hydrodynamics in Integrable Quantum Systems Out of Equilibrium, *Physical Review X* **6**, 041065 (2016).
- [53] Z. Gong, R. Hamazaki, and M. Ueda, Discrete time-crystalline order in cavity and circuit QED systems, *Physical Review Letters* **120**, 040404.
- [54] F. Iemini, A. Russomanno, J. Keeling, M. Schirò, M. Dalmonte, and R. Fazio, Boundary time crystals, *Physical Review Letters* **121**, 035301.
- [55] K. Tucker, B. Zhu, R. J. Lewis-Swan, J. Marino, F. Jimenez, J. G. Restrepo, and A. M. Rey, Shattered time: can a dissipative time crystal survive many-body correlations?, *New Journal of Physics* **20**, 123003 (2018).
- [56] B. Buča, J. Tindall, and D. Jaksch, Non-stationary coherent quantum many-body dynamics through dissipation, *Nature Communications* **10**, 1730.
- [57] B. Zhu, J. Marino, N. Y. Yao, M. D. Lukin, and E. A. Demler, Dicke time crystals in driven-dissipative quantum many-body systems, *New Journal of Physics* **21**, 073028.
- [58] K. Seibold, R. Rota, and V. Savona, Dissipative time crystal in an asymmetric nonlinear photonic dimer, *Physical Review A* **101**, 033839.
- [59] C. Booker, B. Buča, and D. Jaksch, Non-stationarity and dissipative time crystals: spectral properties and finite-size effects, *New Journal of Physics* **22**, 085007.
- [60] H. Alaeian, G. Giedke, I. Carusotto, R. Löw, and T. Pfau, Limit cycle phase and goldstone mode in driven dissipative systems, *Physical Review A* **103**, 013712.
- [61] Y. Nakanishi and T. Sasamoto, Dissipative time crystals originating from parity-time symmetry, *Physical Review A* **107**, L010201.
- [62] A. Cabot, L. S. Muhle, F. Carollo, and I. Lesanovsky, Quantum trajectories of dissipative time crystals, *Physical Review A* **108**, L041303.
- [63] F. Carollo, I. Lesanovsky, M. Antezza, and G. De Chiara, Quantum thermodynamics of boundary time-crystals, *Quantum Science and Technology* **9**, 035024.
- [64] M. de Leeuw, C. Paletta, B. Pozsgay, and E. Vernier, Hidden quasilocal charges and gibbs ensemble in a lindblad system, *Physical Review B* **109**, 054311.
- [65] X. Wu, Z. Wang, F. Yang, R. Gao, C. Liang, M. K. Tey, X. Li, T. Pohl, and L. You, Dissipative time crystal in a strongly interacting Rydberg gas, *Nature Physics* **20**, 1389 (2024).
- [66] Z. Wang, R. Gao, X. Wu, B. Buča, K. Mølmer, L. You, and F. Yang, Boundary Time Crystals Induced by Local Dissipation and Long-Range Interactions, *Physical Review Letters* **135**, 230401 (2025).
- [67] S. Jiang, D. Yuan, W. Jiang, D.-L. Deng, and F. Machado, Prethermal time-crystalline corner modes, *Physical Review Letters* **135**, 110401 ().
- [68] S. Choi, J. Choi, R. Landig, G. Kucsko, H. Zhou, J. Isoya, F. Jelezko, S. Onoda, H. Sumiya, V. Khemani, C. von Keyserlingk, N. Y. Yao, E. Demler, and M. D. Lukin, Observation of discrete time-crystalline order in a disordered dipolar many-body system, *Nature* **543**, 221.
- [69] J. Zhang, P. W. Hess, A. Kyprianidis, P. Becker, A. Lee, J. Smith, G. Pagano, I.-D. Potirniche, A. C. Potter, A. Vishwanath, N. Y. Yao, and C. Monroe, Observation of a discrete time crystal, *Nature* **543**, 217, 1609.08684 [quant-ph].
- [70] H. Keßler, P. Kongkhambut, C. Georges, L. Mathey, J. G. Cosme, and A. Hemmerich, Observation of a Dissipative Time Crystal, *Physical Review Letters* **127**, 043602 (2021), publisher: American Physical Society.
- [71] P. Kongkhambut, H. Keßler, J. Skulte, L. Mathey, J. G. Cosme, and A. Hemmerich, Realization of a periodically driven open three-level dicke model, *Physical Review Letters* **127**, 253601 ().
- [72] A. Kyprianidis, F. Machado, W. Morong, P. Becker, K. S. Collins, D. V. Else, L. Feng, P. W. Hess, C. Nayak, G. Pagano, N. Y. Yao, and C. Monroe, Observation of a prethermal discrete time crystal, *Science* **372**, 1192.
- [73] P. Frey and S. Rachel, Realization of a discrete time crystal on 57 qubits of a quantum computer, 2105.06632 [quant-ph].

- [74] P. Kongkhambut, J. Skulte, L. Mathey, J. G. Cosme, A. Hemmerich, and H. Keßler, Observation of a continuous time crystal, *Science* **377**, 670 (2022).
- [75] Y.-H. Chen and X. Zhang, Realization of an inherent time crystal in a dissipative many-body system, *Nature Communications* **14**, 6161 (2023).
- [76] Y. Jiao, W. Jiang, Y. Zhang, J. Bai, Y. He, H. Shen, J. Zhao, and S. Jia, Observation of multiple time crystals in a driven-dissipative system with rydberg gas, *Nature Communications* **16**, 8767 (2025).
- [77] K. Sacha, Modeling spontaneous breaking of time-translation symmetry, *Physical Review A* **91**, 033617, 1410.3638 [cond-mat].
- [78] C. J. Turner, A. A. Michailidis, D. A. Abanin, M. Serbyn, and Z. Papić, Weak ergodicity breaking from quantum many-body scars, *Nature Physics* **14**, 745 (2018).
- [79] Z.-C. Yang, F. Liu, A. V. Gorshkov, and T. Iadecola, Hilbert-Space Fragmentation from Strict Confinement, *Physical Review Letters* **124**, 207602 (2020).
- [80] L. Gotta, L. Mazza, P. Simon, and G. Roux, Two-fluid coexistence in a spinless fermions chain with pair hopping, *Physical Review Letters* **126**, 206805 (2021).
- [81] M. Serbyn, D. A. Abanin, and Z. Papić, Quantum many-body scars and weak breaking of ergodicity, *Nature Physics* **17**, 675 (2021).
- [82] K. Bidzhiev, M. Fagotti, and L. Zadnik, Macroscopic effects of localized measurements in jammed states of quantum spin chains, *Physical Review Letters* **128**, 130603 (2022).
- [83] L. Zadnik, S. Bocini, K. Bidzhiev, and M. Fagotti, Measurement catastrophe and ballistic spread of charge density with vanishing current, *Journal of Physics A: Mathematical and Theoretical* **55**, 474001 (2022).
- [84] A. Daniel, A. Hallam, J.-Y. Desaulles, A. Hudomal, G.-X. Su, J. C. Halimeh, and Z. Papić, Bridging quantum criticality via many-body scarring, *Physical Review B* **107**, 235108 (2023).
- [85] B. Buča, Unified theory of local quantum many-body dynamics: Eigenoperator thermalization theorems, *Physical Review X* **13**, 031013 (2023).
- [86] W. Deng and Z.-C. Yang, Using models with static quantum many-body scars to generate time-crystalline behavior under periodic driving, *Physical Review B* **108**, 205129 (2023).
- [87] H. Dong, J.-Y. Desaulles, Y. Gao, N. Wang, Z. Guo, J. Chen, Y. Zou, F. Jin, X. Zhu, P. Zhang, H. Li, Z. Wang, Q. Guo, J. Zhang, L. Ying, and Z. Papić, Disorder-tunable entanglement at infinite temperature, *Science Advances* **9**, eadj3822 (2023).
- [88] L. Gotta, S. Moudgalya, and L. Mazza, Asymptotic quantum many-body scars, *Physical Review Letters* **131**, 190401 (2023).
- [89] Z. Guo, B. Liu, Y. Gao, A. Yang, J. Wang, J. Ma, and L. Ying, Origin of hilbert-space quantum scars in unconstrained models, *Physical Review B* **108**, 075124 (2023).
- [90] E. Nicolau, A. M. Marques, R. G. Dias, and V. Ahufinger, Flat band induced local hilbert space fragmentation, *Physical Review B* **108**, 205104 (2023).
- [91] A. Delmonte, A. Romito, G. E. Santoro, and R. Fazio, Quantum effects on the synchronization dynamics of the Kuramoto model, *Physical Review A* **108**, 032219 (2023).
- [92] H. Wilming, T. J. Osborne, K. S. C. Decker, and C. Karrasch, Reviving product states in the disordered Heisenberg chain, *Nature Communications* **14**, 5847 (2023).
- [93] K. Sanada, Y. Miao, and H. Katsura, Quantum many-body scars in spin models with multibody interactions, *Physical Review B* **108**, 155102 (2023).
- [94] G.-X. Su, H. Sun, A. Hudomal, J.-Y. Desaulles, Z.-Y. Zhou, B. Yang, J. C. Halimeh, Z.-S. Yuan, Z. Papić, and J.-W. Pan, Observation of many-body scarring in a Bose-Hubbard quantum simulator, *Physical Review Research* **5**, 023010 (2023).
- [95] S. Bocini and M. Fagotti, Growing schrödinger's cat states by local unitary time evolution of product states, *Physical Review Research* **6**, 033108 (2024).
- [96] M. Fagotti, Quantum jamming brings quantum mechanics to macroscopic scales, *Physical Review X* **14**, 021015 (2024).
- [97] J.-Y. Desaulles, E. J. Gustafson, A. C. Y. Li, Z. Papić, and J. C. Halimeh, Robust finite-temperature many-body scarring on a quantum computer, *Physical Review A* **110**, 042606 (2024).
- [98] R. Shen, F. Qin, J.-Y. Desaulles, Z. Papić, and C. H. Lee, Enhanced many-body quantum scars from the non-hermitian fock skin effect, *Physical Review Letters* **133**, 216601 (2024).
- [99] S. Majidy, Noncommuting charges can remove non-stationary quantum many-body dynamics, *Nature Communications* **15**, 8246 (2024).
- [100] P. H. Harkema, M. Iversen, and A. E. B. Nielsen, Hilbert space fragmentation from lattice geometry, *Physical Review A* **110**, 023301 (2024).
- [101] C. W. Wächtler and J. E. Moore, Topological Quantum Synchronization of Fractionalized Spins, *Physical Review Letters* **132**, 196601 (2024).
- [102] G. Morettini, L. Capizzi, M. Fagotti, and L. Mazza, Transport in a system with a tower of quantum many-body scars, *Physical Review B* **112**, 134314 (2025).
- [103] X.-P. Jiang, M. Xu, X. Yang, H. Hou, Y. Wang, and L. Pan, Robustness of quantum many-body scars in the presence of a markovian bath, *Communications Physics* **9**, 14 (2025).
- [104] Y. H. Kwan, P. H. Wilhelm, S. Biswas, and S. Parameswaran, Minimal hubbard models of maximal hilbert space fragmentation, *Physical Review Letters* **134**, 010411 (2025).
- [105] Y. Meng, S. Lv, Y. Liu, Z. Tan, E. Zhao, and H. Zou, Detecting many-body scars from fisher zeros, *Physical Review Letters* **135**, 070402 (2025).
- [106] F. Yang, H. Yarloo, H.-C. Zhang, K. Mølmer, and A. E. B. Nielsen, Probing hilbert space fragmentation with strongly interacting rydberg atoms, *Physical Review B* **111**, 144313 (2025).
- [107] Y. B. Lev, J. C. Halimeh, and A. Lazarides, Dissipation-stabilized quantum revivals in a non-hermitian lattice gauge theory, 2512.24418 [quant-ph].
- [108] H. Yu, J. Hu, and S.-X. Zhang, Hilbert subspace imprint: a new mechanism for non-thermalization, 2506.11922 [quant-ph].
- [109] T. Pudlik, H. Hennig, D. Witthaut, and D. K. Campbell, Dynamics of entanglement in a dissipative bose-hubbard dimer, *Physical Review A* **88**, 063606 (2013).
- [110] C. Lledó, T. K. Mavrogordatos, and M. H. Szymańska, Driven bose-hubbard dimer under nonlocal dissipation: A bistable time crystal, *Phys. Rev. B* **100**, 054303 (2019).
- [111] C. Lledó and M. H. Szymańska, A dissipative time crystal with or without \mathbb{Z}_2 symmetry

- breaking, *New Journal of Physics* **22**, 075002 (2020), arXiv:2004.02855 [cond-mat, physics:quant-ph].
- [112] C. Liang, Y. Zhang, and S. Chen, Statistical and dynamical aspects of quantum chaos in a kicked bose-hubbard dimer, *Physical Review A* **109**, 033316.
- [113] J. Pi, F. Chen, Q. Liu, L. You, and R. Lü, The dynamics of an open Bose–Hubbard dimer with effective asymmetric coupling, *The European Physical Journal B* **97**, 26 (2024).
- [114] B. Buča and T. Prosen, A note on symmetry reductions of the Lindblad equation: transport in constrained open spin chains, *New Journal of Physics* **14**, 073007 (2012).
- [115] C.-M. Halati, A. Sheikhan, and C. Kollath, Breaking strong symmetries in dissipative quantum systems: Bosonic atoms coupled to a cavity, *Physical Review Research* **4**, L012015 (2022).
- [116] S. Diehl, A. Tomadin, A. Micheli, R. Fazio, and P. Zoller, Dynamical Phase Transitions and Instabilities in Open Atomic Many-Body Systems, *Physical Review Letters* **105**, 015702 (2010).
- [117] M.-J. Hwang, P. Rabl, and M. B. Plenio, Dissipative phase transition in the open quantum Rabi model, *Physical Review A* **97**, 013825 (2018).
- [118] S. Dutta, An introduction to markovian open quantum systems, 2510.26530 [quant-ph].
- [119] H. Yoshida and R. Hamazaki, Theory of Steady States for Lindblad Equations beyond Time-Independence: Classification, Uniqueness and Symmetry (2026), arXiv:2602.13095 [quant-ph].
- [120] W. Casteels and C. Ciuti, Quantum entanglement in the spatial-symmetry-breaking phase transition of a driven-dissipative bose-hubbard dimer, *Phys. Rev. A* **95**, 013812 (2017).
- [121] W. Casteels, R. Fazio, and C. Ciuti, Critical dynamical properties of a first-order dissipative phase transition, *Phys. Rev. A* **95**, 012128 (2017).
- [122] V. V. Albert, Lindbladians with multiple steady states: theory and applications (2018), arXiv:1802.00010 [quant-ph].
- [123] D. Manzano, A short introduction to the Lindblad Master Equation, *AIP Advances* **10**, 025106 (2020), arXiv:1906.04478 [cond-mat, physics:quant-ph].
- [124] M. Stefanini, A. A. Ziolkowska, D. Budker, U. Poschinger, F. Schmidt-Kaler, A. Browaeys, A. Imamoglu, D. Chang, and J. Marino, Is Lindblad for me? (2025), version Number: 1.
- [125] See Supplemental Material.
- [126] M. Esencan, Github: Time crystals as self-correcting noiseless qubits numerical data and simulation code, <https://github.com/mertesencan/time-crystals-oscillating-qubits> (2026).
- [127] J. R. Johansson, P. D. Nation, and F. Nori, Qutip: An open-source python framework for the dynamics of open quantum systems, *Computer Physics Communications* **183**, 1760 (2012).
- [128] L.-M. Duan and G.-C. Guo, Preserving Coherence in Quantum Computation by Pairing Quantum Bits, *Physical Review Letters* **79**, 1953 (1997).
- [129] P. Zanardi and M. Rasetti, Noiseless Quantum Codes, *Physical Review Letters* **79**, 3306 (1997).
- [130] D. A. Lidar, I. L. Chuang, and K. B. Whaley, Decoherence-Free Subspaces for Quantum Computation, *Physical Review Letters* **81**, 2594 (1998).
- [131] A. E. B. Nielsen, Fighting decoherence in a continuous two-qubit odd- or even-parity measurement with a closed-loop setup, *Physical Review A* **81**, 012307 (2010).
- [132] M. A. Nielsen and I. L. Chuang, *Quantum Computation and Quantum Information: 10th Anniversary Edition*, 1st ed. (Cambridge University Press, 2012).
- [133] M. Mirrahimi, Z. Leghtas, V. V. Albert, S. Touzard, R. J. Schoelkopf, L. Jiang, and M. H. Devoret, Dynamically protected cat-qubits: a new paradigm for universal quantum computation, *New Journal of Physics* **16**, 045014 (2014).
- [134] M. B. Plenio and P. L. Knight, The quantum-jump approach to dissipative dynamics in quantum optics, *Rev. Mod. Phys.* **70**, 101 (1998).
- [135] M. P. Zaletel, M. Lukin, C. Monroe, C. Nayak, F. Wilczek, and N. Y. Yao, *Colloquium* : Quantum and classical discrete time crystals, *Reviews of Modern Physics* **95**, 031001 (2023).
- [136] F. Minganti, A. Biella, N. Bartolo, and C. Ciuti, Spectral theory of liouvillians for dissipative phase transitions, *Physical Review A* **98**, 042118 (2018).
- [137] H. Taheri, A. B. Matsko, T. Herr, and K. Sacha, Dissipative discrete time crystals in a pump-modulated kerr microcavity, *Communications Physics* **5**, 159.
- [138] M. Mamaev, L. C. G. Góvia, and A. A. Clerk, Dissipative stabilization of entangled cat states using a driven Bose-Hubbard dimer, *Quantum* **2**, 58 (2018).
- [139] C. Chamberland, K. Noh, P. Arrangoiz-Arriola, E. T. Campbell, C. T. Hann, J. Iverson, H. Putterman, T. C. Bohdanowicz, S. T. Flammia, A. Keller, G. Refael, J. Preskill, L. Jiang, A. H. Safavi-Naeini, O. Painter, and F. G. S. L. Brandão, Building a fault-tolerant quantum computer using concatenated cat codes, *PRX Quantum* **3**, 010329, 2012.04108 [quant-ph].
- [140] J. O’Sullivan, O. Lunt, C. W. Zollitsch, M. L. W. The-walt, J. J. L. Morton, and A. Pal, Signatures of discrete time crystalline order in dissipative spin ensembles, *New Journal of Physics* **22**, 085001.

Supplemental Material for “Dissipative Time Crystals as Self-Correcting Qubits”

Mert Esencan,¹ A. I. Lvovsky,¹ and Berislav Buča^{2,3,1}

¹Clarendon Laboratory, University of Oxford, Parks Road, OX1 3PU, Oxford, United Kingdom

²Université Paris-Saclay, CNRS, LPTMS, 91405, Orsay, France

³Niels Bohr Institute, University of Copenhagen, Blegdamsvej 17, 2100, Copenhagen, Denmark

1. MEAN FIELD DYNAMICS IN THE SEMICLASSICAL LIMIT

Treating both the bonding mode and antibonding mode as coherent states [1], in the semiclassical limit as $\langle a_k \rangle \approx \alpha_k$, we get:

$$\frac{d\alpha_B}{dt} = (i\Delta + iJ - \gamma)\alpha_B - iU(\alpha_B|\alpha_B|^2 + 2|\alpha_A|^2\alpha_B + \alpha_A^2\alpha_B^*) - \sqrt{2}iF, \quad (\text{S1})$$

$$\frac{d\alpha_A}{dt} = i(\Delta - J)\alpha_A - iU(\alpha_B^2\alpha_A^* + 2|\alpha_B|^2\alpha_A + \alpha_A|\alpha_A|^2). \quad (\text{S2})$$

Solving these coupled equations with the parameters $J = 1.1$, $\Delta = 0.8$, $U = 1$, $F = 1.8$, $\gamma = 1$ (the parameter set we use repeatedly in the main text) we get the steady state solution $\alpha_B = 1.269$ and $\alpha_A = 0$. Scaling $F \rightarrow \tilde{F}$ and $U \rightarrow \tilde{U}$ leads to the same equations, thus omitted here. Solutions of α_B for different F can be found in Fig. S1 (black lines). A sudden jump in the coherent amplitude is observed at the dissipative phase transition region at $\tilde{F} = 0.93$.

The steady state solution is realized only when initialized $\alpha_A = 0$. Otherwise, α_A persistently oscillates with a small amplitude, crucial for our time crystalline dynamics. The bonding α_B also oscillates around its steady state with a small amplitude, which scales quadratically with respect to α_A , due to the coupling terms in (S2). To calculate the oscillation frequency, we consider the evolution of α_A according to Eq. (S2), assuming constant α_B and neglecting higher-order terms in α_A :

$$\begin{pmatrix} \frac{d\alpha_A}{dt} \\ \frac{d\alpha_A^*}{dt} \end{pmatrix} = V \begin{pmatrix} \alpha_A \\ \alpha_A^* \end{pmatrix}, \quad (\text{S3})$$

where

$$V = \begin{pmatrix} (J - \Delta) + 2U|\alpha_B|^2 & U\alpha_B^2 \\ -U\alpha_B^{*2} & -(J - \Delta) - 2U|\alpha_B|^2 \end{pmatrix}.$$

The oscillation frequency is then the absolute value of the eigenvalues of matrix V :

$$\omega_A = \sqrt{(U|\alpha_B|^2 - \Delta + J)(3U|\alpha_B|^2 - \Delta + J)}. \quad (\text{S4})$$

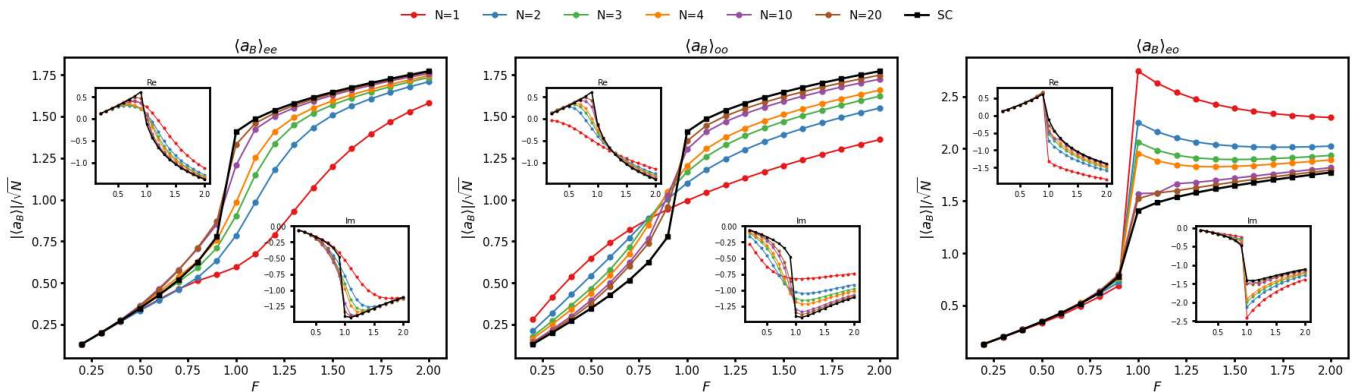


FIG. S1: Bonding mode expectations $\langle a_B \rangle$ from Liouvillian eigenvectors r_{ee} , r_{oo} and r_{eo} plotted against semiclassical steady states calculated from Eq. (S1) and Eq. (S2) r_{oe} is excluded as it is simply the Hermitian conjugate of r_{eo} .

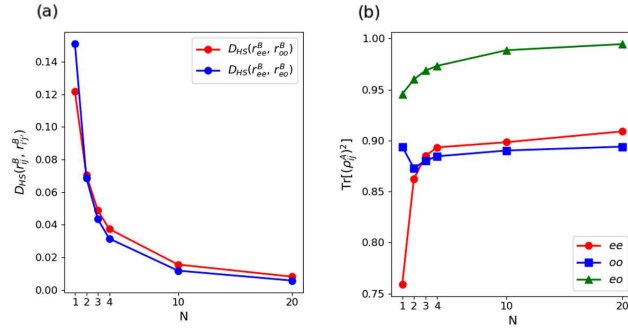


FIG. S2: (a) The Hilbert-Schmidt distances of the bonding modes within the right eigenvectors of different sectors for $F = 1.8$. The modes become similar towards the thermodynamic limit. (b) Purities of the eigenoperators for the same system drive.

2. QUANTUM EIGENOPERATOR CHARACTERISTICS

We now compare the semiclassical calculations with the quantum treatment. We calculate the amplitude expectation values $\langle a_B \rangle$ from the eigenoperators of the Liouvillian. It is visible in Fig. S1 that the amplitudes for all four eigenoperators become close to the mean-field predictions towards the thermodynamic limit. Further, we show in Fig. S2 (a) the bonding mode partial-trace eigenoperators $r_{ij}^B = \text{Tr} r_{ij}$ have decreasing Hilbert-Schmidt (HS) distances with increasing N .

On the other hand, tracing out the bonding mode to investigate the antibonding mode, we see in Fig. S2 while the purity of r_{eo}^A becomes 1 in the thermodynamic limit, while the other eigenoperators r_{ee}^A and r_{oo}^A do not appear to become pure — indicating that the noiseless subsystem is not contained in the antibonding mode (see the main text).

3. TREATING DEPHASING AS A PERTURBATION IN THE LEADING ORDER

To estimate the effect of global dephasing in the leading order, we apply perturbation theory. We consider the perturbed Liouvillian of the form

$$\mathcal{L} = \mathcal{L}_0 + \alpha \mathcal{L}_1, \quad (\text{S5})$$

where $\alpha \ll 1$ is a small parameter. Right and left eigenvectors of \mathcal{L}_0 obey

$$\mathcal{L}_0 |r_j^{(0)}\rangle\rangle = \lambda_j^{(0)} |r_j^{(0)}\rangle\rangle, \quad \mathcal{L}_0^\dagger |l_j^{(0)}\rangle\rangle = \lambda_j^{(0)*} |l_j^{(0)}\rangle\rangle, \quad (\text{S6})$$

with Hilbert-Schmidt normalization

$$\langle\langle l_j^{(0)} | r_k^{(0)} \rangle\rangle \equiv \text{Tr} \left[(l_j^{(0)})^\dagger r_k^{(0)} \right] = \delta_{jk}. \quad (\text{S7})$$

We now look for perturbed eigenvalues and eigenvectors of \mathcal{L} in the form of power series in α :

$$\lambda_j = \lambda_j^{(0)} + \alpha \lambda_j^{(1)} + O(\alpha^2), \quad (\text{S8})$$

$$|r_j\rangle\rangle = |r_j^{(0)}\rangle\rangle + \alpha |r_j^{(1)}\rangle\rangle + O(\alpha^2). \quad (\text{S9})$$

Inserting this expansion into the perturbed eigenvalue equation and keeping terms up to first order in α gives

$$(\mathcal{L}_0 + \alpha \mathcal{L}_1)(|r_j^{(0)}\rangle\rangle + \alpha |r_j^{(1)}\rangle\rangle) = (\lambda_j^{(0)} + \alpha \lambda_j^{(1)})(|r_j^{(0)}\rangle\rangle + \alpha |r_j^{(1)}\rangle\rangle) + O(\alpha^2). \quad (\text{S10})$$

Expanding and grouping terms by powers of α yields in the zeroth order:

$$\mathcal{L}_0 |r_j^{(0)}\rangle\rangle = \lambda_j^{(0)} |r_j^{(0)}\rangle\rangle, \quad (\text{S11})$$

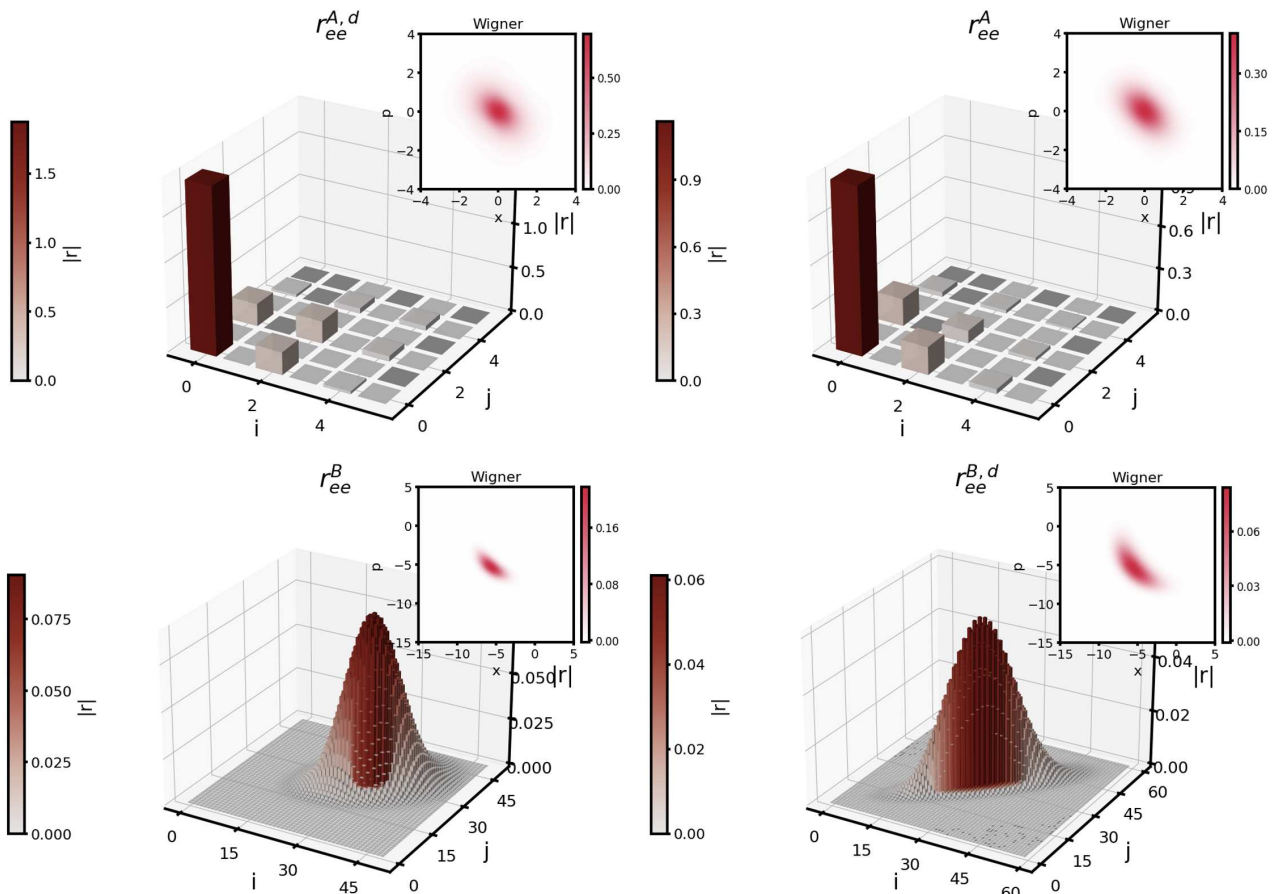


FIG. S3: (a) Eigenoperators in the presence (superscript d) and absence of dephasing for $N = 10$ and $\tilde{F} = 1.8$. A larger Fock cutoff of $K = 60$ was used to get the dephased state, while $K = 50$ was used for the original Liouvillian.

which is just the unperturbed eigenvalue equation. The terms proportional to α on the other hand give us in first (leading) order

$$\mathcal{L}_0|r_j^{(1)}\rangle + \mathcal{L}_1|r_j^{(0)}\rangle = \lambda_j^{(0)}|r_j^{(1)}\rangle + \lambda_j^{(1)}|r_j^{(0)}\rangle. \quad (\text{S12})$$

Rearranging, we get

$$(\mathcal{L}_0 - \lambda_j^{(0)})|r_j^{(1)}\rangle = -(\mathcal{L}_1 - \lambda_j^{(1)})|r_j^{(0)}\rangle. \quad (\text{S13})$$

To extract $\lambda_j^{(1)}$ we now left-multiply Eq. (S13) by $\langle\langle l_j^{(0)}|$. The left-hand side of Eq. (S13) vanishes, and we obtain

$$0 = -\langle\langle l_j^{(0)}|(\mathcal{L}_1 - \lambda_j^{(1)})|r_j^{(0)}\rangle\rangle, \quad (\text{S14})$$

and therefore

$$\langle\langle l_j^{(0)}|\mathcal{L}_1|r_j^{(0)}\rangle\rangle = \lambda_j^{(1)}\langle\langle l_j^{(0)}|r_j^{(0)}\rangle\rangle. \quad (\text{S15})$$

Using the normalization $\langle\langle l_j^{(0)}|r_j^{(0)}\rangle\rangle = 1$, we finally obtain the first-order correction

$$\lambda_j^{(1)} = \langle\langle l_j^{(0)}|\mathcal{L}_1|r_j^{(0)}\rangle\rangle = \text{Tr}\left[\langle l_j^{(0)}|^\dagger \mathcal{L}_1|r_j^{(0)}\rangle\right]. \quad (\text{S16})$$

This is the Liouvillian analogue of first-order perturbation theory for Hamiltonian eigenvalues. The real and imaginary parts of $\lambda^{(1)}$ have clear physical meanings: $-\text{Re}\{\lambda^{(1)}\}$ is the additional decay rate and $\text{Im}\{\lambda^{(1)}\}$ is the frequency shift due to dephasing. The altered states can be found in Fig. S3.

4. COMPUTATIONAL METHODS

We are operating in the doubled Hilbert space (Fock-Liouville space) where density matrices are D dimensional column vectors, and the Liouvillian is a D by D matrix. In a bosonic system, D should be infinite. However to be able to perform any numerical analysis, we need to work with finite matrices. As such we truncate these systems in the Fock basis.

If we choose the cutoff point at $|K - 1\rangle$, then our coupled state of two modes is a column vector with K^2 elements, its corresponding density matrix is K^2 by K^2 , and in the doubled Hilbert space is a column vector of size K^4 . Thus the Liouvillian we are trying to diagonalize is a K^4 by K^4 matrix. As one can see, the computational requirements increase dramatically with the Fock truncation limit, severely limiting one to study large systems.

The model we study in the lab basis is governed by the Hamiltonian

$$\hat{H} = F(\hat{a}_1 + \hat{a}_2 + \hat{a}_1^\dagger + \hat{a}_2^\dagger) - \Delta\hat{a}_1^\dagger\hat{a}_1 - \Delta\hat{a}_2^\dagger\hat{a}_2 - J(\hat{a}_1^\dagger\hat{a}_2 + \hat{a}_1\hat{a}_2^\dagger) + \sum_{1,2} (U\hat{a}_i^\dagger\hat{a}_i^\dagger\hat{a}_i\hat{a}_i) \quad (\text{S17})$$

for modes a_1 and a_2 . If we had chosen this basis, we would have used the same truncation for both modes. However we choose to work in the beam splitter basis, which reduces our computational requirements thanks to the microscopic amplitude of the antibonding mode. We set $K_A = 6$ for all N . For the bonding mode, we use $K_A = [14, 20, 24, 30, 50, 100]$ for $N = [1, 2, 3, 4, 10, 20]$. Computations for $N \leq 4$ were performed with exact diagonalization, where all eigenstates were found. For $N = 10, 20$ we used sparse diagonalization, where we diagonalized the Liouvillian matrices using ARPACK methods [2, 3]. We computed only the leading eigenpairs, targeting the eigenvalues with largest real part (LR) corresponding to longest-lived modes. Convergence was verified by increasing the Fock cutoffs K_B and the Krylov dimension until the relevant eigenvalues and observables were stable, in addition to checking the continuity of eigenoperators with respect to small changes of \tilde{F} . The sparse solver was unable to converge for the eigenstates around the transition point at $\tilde{F} = 0.93$.

-
- [1] C. Lledó, T. K. Mavrogordatos, and M. H. Szymańska, Phys. Rev. B **100**, 054303 (2019), URL <https://link.aps.org/doi/10.1103/PhysRevB.100.054303>.
 - [2] J. R. Johansson, P. D. Nation, and F. Nori, Computer Physics Communications **183**, 1760 (2012).
 - [3] R. B. Lehoucq, D. C. Sorensen, and C. Yang, *ARPACK Users' Guide: Solution of Large-Scale Eigenvalue Problems with Implicitly Restarted Arnoldi Methods* (SIAM, Philadelphia, 1998).